

EVALUATION OF DELAMINATION AND BENDING PERFORMANCE OF COMPOSITE CLT REINFORCED WITH CFRP

Yo-Jin Song

Senior Researcher
Division of Forest Material Science & Engineering
Kangwon National University
1 Gangwondaehakgil
Chuncheon-Si 24341, Republic of Korea
E-mail: syj85@kangwon.ac.kr

In-Hwan Lee

PhD Student
E-mail: kvest31@naver.com

Da-Bin Song

Graduate Students
E-mail: whswk526@naver.com

*Soon-Il Hong**

Professor
Division of Forest Material Science & Engineering
Kangwon National University
1 Gangwondaehakgil
Chuncheon-Si 24341, Republic of Korea
E-mail: hongsi@kangwon.ac.kr

(Received January 2019)

Abstract. To develop a high-performance, lightweight, cross-laminated timber (CLT) floor, this study tested the delamination performance between carbon fiber-reinforced plastic (CFRP) and CLT and the bending performance of a CFRP composite CLT that was differently reinforced according to the shape of the CFRP. The test results showed that the soaking and boiling delamination between CLT and CFRP of the CFRP composite CLT produced by spreading a polyurethane adhesive at 300 g/m² were both less than 5%, satisfying the Korean standard. Furthermore, the composite CLT (3 ply) of which the entire outer surface of the tension laminae was reinforced with a CFRP plate (thickness: 1.2 mm) showed a mean MOE and a mean MOR higher by 27% and 48%, respectively, than those of the unreinforced CLT (3ply). Furthermore, even though the weight of this CFRP composite CLT was smaller than that of 5ply CLT by approximately 40%, its bending moment was measured higher by 14% than that of the 5 ply CLT (thickness: 175 mm) fabricated by limited state design as specified in PRG-320.

Keywords: Cross-laminated timber (CLT), Japanese larch, composite CLT floor, delamination test, bending strength, carbon fiber-reinforced plastic (CFRP).

INTRODUCTION

Cross-laminated timber (CLT) is an engineered timber panel produced by cross-lamination of three layers or more (in general, 3, 5, 7, or higher layers) of visually or mechanically graded laminae

by an adhesive or mechanical method. Because of the characteristics of the manufacturing method, CLT panels can produce panels with a large cross section, and they can be used as structural materials for floor, wall, and roof. In particular, when CLT is used as roof, it requires enhanced bending performance (Song 2018). For this reason, studies have been conducted on the flexural performance

* Corresponding author

of CLT according to various conditions, such as the thickness of the tree and the tree species, of the laminae (Gülzow et al 2011; Hochreiner et al 2014; Flaig and Blaß 2014; Park et al 2016; Sikora et al 2016; Liao et al 2017; He et al 2018), and the studies predicted the bending performance using various tests (Steiger et al 2012; Okabe et al 2014). Furthermore, the studies used engineered woods such as plywood and laminated strand lumber instead of solids in the middle layer or applied 45 degrees instead of 90 degrees for longitudinal and orthogonal laminae to improve the degradation of bending performance of CLT by rolling shear (Choi et al 2015; Wang et al 2015; Buck et al 2016).

CLT has good constructability because of a specific gravity that is lower by approximately 1/5 than that of concrete; as a result, it can shorten construction period and save construction cost (Yin 2018). However, among the elements of CLT buildings, the CLT floor is usually designed thicker than the CLT wall because of the higher bending performance requirements. In addition, heavy topping such as concrete is added to the top of CLT for fireproofing and prevention of floor noise general. Thus, the weight of the CLT floor occupies a large part in a CLT building. This increase in floor weight becomes an additional weight for the lateral load of earthquake. Furthermore, if a large amount of wood is used when producing CLT floor with a large cross section, it has low economical advantage in South Korea where the mass timber construction market is small. Therefore, in the global trend of increasing high-rise buildings using CLT, we should achieve the seismic performance and improve the constructability and economic efficiency by lowering the self-weight of buildings, which becomes an additional load to the lateral load of earthquake, through the design of lightweight CLT floors. In this respect, the prices of structural materials can be reduced by decreasing the use of woods through carbon fiber-reinforced plastic (CFRP) reinforcement because the reinforcement and lightweight production using CFRP have been applied to solid woods and glulams and their effects on wooden structures have been proven. It is expected that the lightweight production of CLT-concrete floors will provide bending performance

and improve constructability and economic efficiency while at the same time reducing the self-weight of the CLT structure systems. Therefore, in this study, the appropriate adhesive between CLT and CFRP was reviewed through the delamination test of composite CLT reinforced with CFRP. In addition, the bending performance was verified by performing 4-point bending load test for composite CLTs that were reinforced differently by CFRP plate and CFRP bar.

MATERIALS AND METHODS

Material Preparation

In this study, larch (*Larix kaempferi* Carr.) laminae with an air-dried specific gravity of 0.57 (± 0.02) and an air-dried MC of 12% ($\pm 2\%$) were used. In the delamination performance evaluation, laminae with a size of 27 mm (t) \times 89 mm (w) were used. In the bending performance evaluation, laminae with a size of 35.5 mm (t) \times 140 mm (w) were used. For reinforcements, CFRP plates with a size of 1.2 mm (t) \times 100 mm (w) \times 2500 mm (l) and rectangular CFRP rods with a size of 6.5 mm (t) \times 12.5 mm (w) \times 2500 mm (l) were used (Fig 1). Both reinforcements were pultruded with epoxy (EP) resin, and the MOE and tensile strength were 487,000 MPa and 2557 MPa, respectively (Park 2009).

Evaluation of Delamination Performance

Adhesives. The bonding performance of CLT for various adhesives satisfied the respective standards in previous studies (Kim et al 2013; Gong et al 2016; Song and Hong 2016; Lu et al 2018). Therefore, this study attempted to verify the bond performance between CLT and CFRP according to the adhesive type and the changing adhesive spread

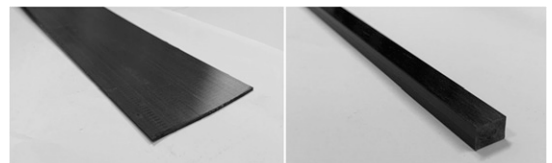


Figure 1. Carbon fiber-reinforced plastic (CFRP) plate and CFRP bar.

of each adhesive. Four types of adhesives were used: type 2 polyvinyl acetate (PVAc), phenol-resorcinol formaldehyde (PRF), EP, and type 1 polyurethane (PUR). The detailed information about the adhesives is outlined in Table 1.

Manufacturing of delamination test specimens. The CFRP composite CLT for delamination performance evaluation was laminated in three layers. The MOEs of the laminae were randomly set. For the delamination test to involve rigorous conditions between CLT and CFRP, a CFRP plate was inserted between the middle and outer laminae instead of on the surface of the outer lamina. Adhesives perform differently depending on the bonding conditions. In this study, mix ratio and assemble time were applied according to the technical data sheet (TDS) of each adhesive as shown in Table 1. The adhesive was applied only to the flat surface of the laminae and not to the sides. PVAc, PRF, and PUR were applied at 200 g/m², 300 g/m², and 400 g/m², respectively, for each adhesive. In the case of EP, it was not applied properly when it was applied at 200 g/m² because of the high density of the product. Thus, the applied amount was increased to 300 g/m², 400 g/m², and 500 g/m². The recommended press pressure for the TDS differed somewhat for each adhesive from 0.8 MPa to 1.0 MPa. However, considering the specific gravity of wood, a press pressure of 1.0 MPa was applied equally to the composite CLT because the laminae and reinforcement must be pressed simultaneously for economic feasibility. The composite CLT was cured at 23°C without any separation of adhesives, whereas the manufactured composite CLTs were cured for more than 1 wk at 23°C. The CFRP composite CLTs were sampled in the size of 75 mm (*w*) × 75 mm (*l*) × 82 mm (*h*) as shown in Fig 2 in accordance with KS F 3021. The adhesive layer between the sides of laminae was not included in the delamination specimen (KS F

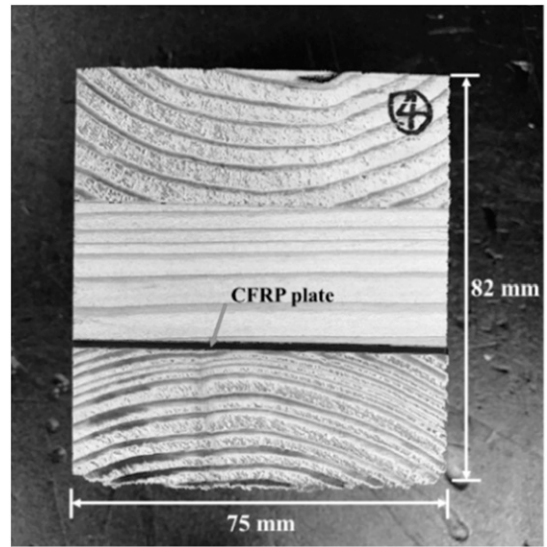


Figure 2. Size of delamination specimens.

3021). The delamination specimen fabrication plan is outlined in Table 2.

Delamination test. The delamination performance test was performed by soaking and boiling delamination tests in accordance with KS F 2160 and KS F 3021. The soaking delamination test method was as follows. The specimen was soaked in water at normal temperature for 24 h and then put in a dry oven at 70 ± 3°C. After drying for 24 h, when the water content after drying became lower than the water content before drying, the delamination length was measured. For boiling delamination test, the specimen was soaked in boiling water for 4 h and then in water at normal temperature for 1 h. After that, in the same way as the soaking delamination test, the specimen was dried in a dry oven at 70 ± 3°C for more than 23 h. When the water content after drying became lower than the water content before drying, the delamination length was measured (KS F 3201; KS F 2160). Delamination length was not

Table 1. Information and properties of adhesives.

Adhesive	Mix ratio (resin: hardener)	Assembly time (min)	Viscosity (mPa. s)	Density (g/cm ³)	Color
Polyvinyl acetate	10: 1	60 (30°C)	6000-7500	1.1	Ivory white
Phenol-resorcinol formaldehyde	10: 1.5	120 (25°C)	300-1000	1.2	Reddish brown
Epoxy	3: 1	90 (20°C)	Thixotropy	1.7	Light gray
Polyurethane	1-component	20 (23°C)	~2000 (23°C)	1.2	Light beige

Table 2. Program of delamination test.

Adhesive	Reinforcement	Press pressure (MPa)	Adhesive spread (g/m ²)	Delamination test	Series	Number of specimens			
Polyvinyl acetate	Carbon fiber-reinforced plastic	1.0	200	Soaking	PV2S	10			
				Boiling	PV2B	10			
			300	Soaking	PV3S	10			
				Boiling	PV3B	10			
			400	Soaking	PV4S	10			
				Boiling	PV4B	10			
			Phenol-resorcinol formaldehyde			200	Soaking	PR2S	10
							Boiling	PR2B	10
300	Soaking	PR3S				10			
	Boiling	PR3B				10			
400	Soaking	PR4S				10			
	Boiling	PR4B				10			
Epoxy						300	Soaking	EP3S	10
							Boiling	EP3B	10
			400	Soaking	EP4S	10			
				Boiling	EP4B	10			
			500	Soaking	EP5S	10			
				Boiling	EP5B	10			
			Polyurethane			200	Soaking	PU2S	10
							Boiling	PU2B	10
300	Soaking	PU3S				10			
	Boiling	PU3B				10			
400	Soaking	PU4S				10			
	Boiling	PU4B				10			

measured for the adhesive layer between the woods, but only for adhesive layers between the wood and CFRP plate. The delamination ratio was calculated by substituting the measured delamination length in the following Eq 1:

$$\text{Delam}_{\text{wood-CFRP}} = \frac{l_{\text{wood-CFRP,delam}}}{l_{\text{wood-CFRP,glueline}}} \times 100, \tag{1}$$

$$\begin{aligned} \text{Delam}_{\text{wood-CFRP}} &= \text{Total delamination}(\%), \\ l_{\text{wood-CFRP,delam}} &= \text{Total delamination length (mm)}, \end{aligned}$$

$$\begin{aligned} l_{\text{wood-CFRP, glueline}} &= \text{Sum of the perimeters of glue lines of wood} \\ &\text{- CFRP in a delamination specimen (mm)}. \end{aligned}$$

Evaluation of Bending Performance

Manufacturing of bending test specimens. When fabricating the bending test specimen, the adhesive

that showed the best delamination performance between CFRP and CLT in section 2.2. “*Evaluation of delamination performance*” was used. The specimen was fabricated in three layers and the MOEs of the laminae were randomly set. The adhesive was applied to the flat surface of the laminae, and not to the sides. The size of the specimen was 106.5 mm (*t*) × 275.0 mm (*w*) × 2500 mm (*l*). Three types of series were fabricated according to the presence/absence of reinforcement and the reinforcement method. Series-A is an unreinforced specimen as shown in Fig 3. Series-B is a specimen reinforced with CFRP plates on the entire outer surface of the tension member of CLT as shown in Fig 4 (volume ratio of reinforcement: 0.011). Series-C is a specimen

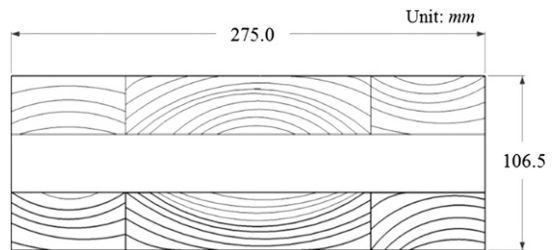


Figure 3. Schematic diagram of cross section of Series-A.

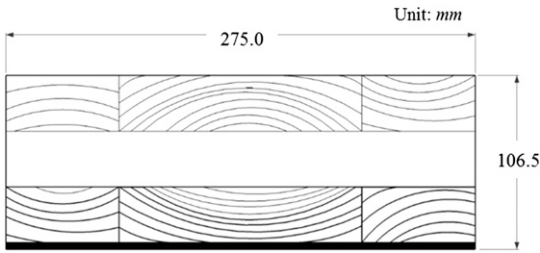


Figure 4. Schematic diagram of cross section of Series-B.

reinforced with CFRP bars inserted into and bonded with three grooves (15 mm [t] × 8 mm [w] × 2500 mm [l]) machined on the outer surface of the tension member of CLT as shown in Fig 5 (volume ratio of reinforcement: 0.008). Five specimens were fabricated for each series.

Bending Test

The bending test was performed in the major strength direction of the CLT floor. For the bending test, 4-point load was used as shown in Fig 6 in accordance with prEN 16351 (2015). The span-to-depth ratio was 22.5:1 and the distance between the two loading points was six times the thickness of the CLT panel. The global deformation of the CLT by the vertical load was measured with the displacement transducer located at the center. The displacement transducers installed at 2.5 h to either side from the center of the specimen measured the local deformation. The loading rate was 13 mm/min and the maximum load was reached within 5 min after the

start of the test. The MOE and MOR were calculated using Eqs 2 and 3.

$$MOE = \frac{\Delta Pa(3l^2 - 4a^2)}{48I\Delta V} x, \tag{2}$$

$$MOR = \frac{3P_{max}(l - s)}{2bh^2}, \tag{3}$$

P_{max} = Maximum load (N),
 ΔP = Proportional limit load (N),

ΔV = Proportional limit deformation (mm),
 l = Span (mm),

s = Distance between the load (mm),

b = Specimen width (mm),

h = Specimen thickness (mm),

a = Distance between the supporting and loading point (mm),

I = Geometrical moment of inertia.

RESULTS AND DISCUSSION

Delamination Performance of CFRP Composite CLT

Figure 7 shows the soaking and delamination test results between CLT and CFRP. In the case of PVAc, the soaking delamination of Series-PV3 and Series-PV4 approached 5%, but the boiling delamination was very high. Compared with

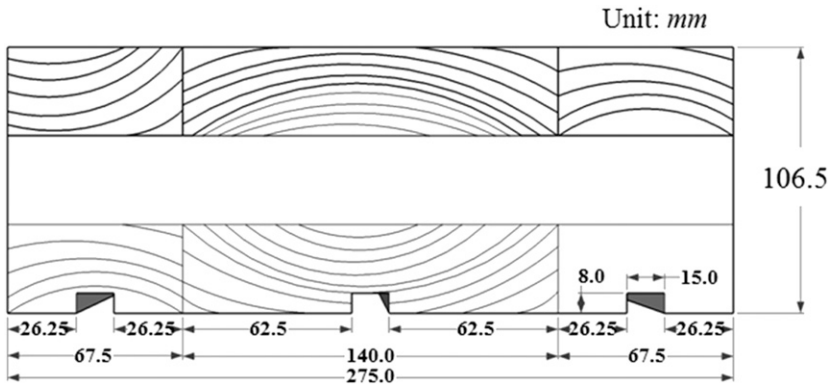


Figure 5. Schematic diagram of cross section of Series-C.

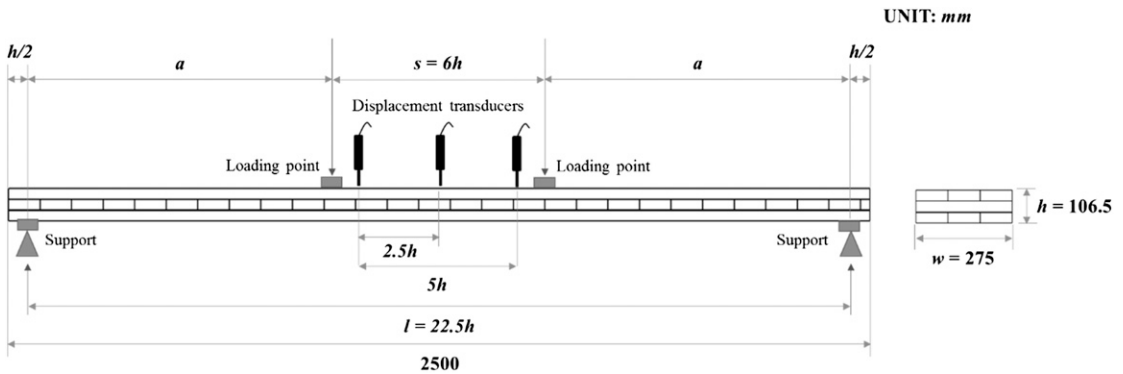


Figure 6. Test setup for bending perpendicular to the plane of cross-laminated timber.

other adhesives, PUR had an excellent bonding performance between CLT and CFRP. In particular, the soaking and boiling delamination of Series-PU3 were 3.0% and 0%, respectively, satisfying the KS F standard of 5%. EP did not satisfy the standard, but the resistance performance against soaking and boiling was not large. In the case of PRF, the delamination in the boiling delamination test, which is a harsher test environment than the soaking delamination test, was measured lower. This tendency was confirmed by Kim who evaluated the delamination performance between laminated timber and CFRP (Kim 2012).

In the drying process, late wood has a greater density than early wood, so late wood shrinks more and “cupping” occurs where the wood is

bent reversely to the direction of the annual ring on the cross section. The arrows in Fig 8 show the shrinkage direction of the lamina by cupping during drying. In the case of Series-PU3, the bonding performance between wood and CFRP was maintained even if the middle lamina shrank toward the center of the specimen by cupping. For the other series, delamination occurred because the shrinkage stress of the middle lamina was greater than the wood-CFRP bonding strength. However, Lu et al reported that using coupling agents made of hydroxymethylated resorcinol or N, N-dimethylformamide can improve the bonding performance (Lu et al 2018). Therefore, the delamination performance could be improved by using these coupling agents even if the adhesive did not satisfy the standard in this study.

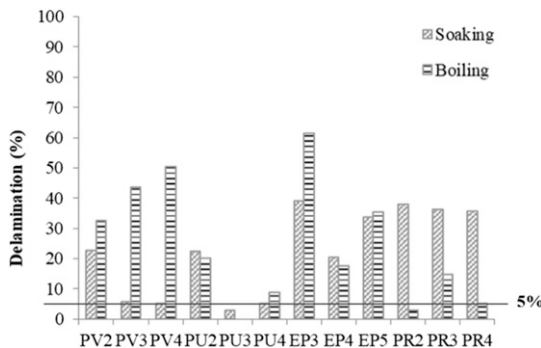


Figure 7. Wood-wood and wood-carbon fiber-reinforced plastic delamination according to the adhesive and adhesive spread.

Bending Performance of CFRP Composite CLT Floor

Load-global deformation curves. Figure 9 shows the load-global deformation curve for the bending test. The mean maximum load of Series-A was 45,785.6 N. Most load-global deformation curves were close to a straight line, until the first failure occurred in the tension member. After that, the load increased again, and the second failure occurred in the middle lamina. The mean maximum load of Series-B was 67,825.8 N. Unlike Series-A, Series-B failures never occurred in the reinforced outer lamina. Rather, the first failure sometimes occurred

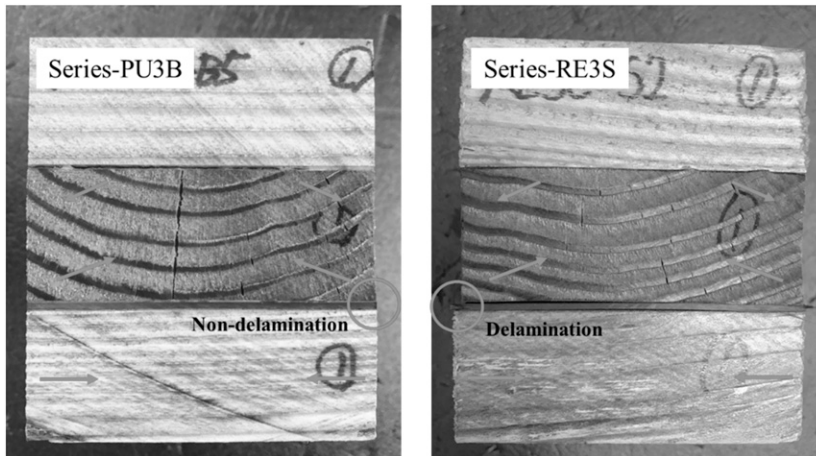


Figure 8. Contraction direction of laminae by cupping.

because of the local rolling shear or tension perpendicular failure in the cross-banded middle lamina (Fig 10). For Series-B specimens, the load at failure was significantly higher than Series-A and Series-C specimens (Fig 9). After the first failure, a failure occurred in the middle lamina at the maximum load, and then the load decreased significantly. The mean maximum load of Series-C was 49,235.2 N. Series-C specimens also had a similar multi-peaked load–global deformation curves as observed with Series-A specimens.

Bending strength properties. The bending performances of the composite CLTs are listed in Table 3. The mean MOE_{Global} and MOR of Series-A were measured at 10,693.2 MPa and 38.6 MPa, respectively. The MOE_{Global} and MOR of Series-B of which the entire outer surface of the tension member was reinforced with a CFRP plate were 13,593.7 MPa and 57.2

MPa, respectively, which were higher by 27% and 48%, respectively, than those of Series-A, showing a positive reinforcing effect. These increase rates are greater than that of the reinforcement by GFRP plate in the previous study, which was 20% for MOE and 31% for MOR (Song and Hong 2018). The reinforcement by CFRP plate had a greater contribution to the increase in MOR than MOE of the larch CLT, and this tendency also appeared in the study by Park (2009) and Raftery and Harte (2011). The reason is that although FRP plates are not as rigid as metal, when the tension side is reinforced, it suppresses the failure of the tension lamina and causes a failure of the middle lamina or the compressive lamina of the compressive side (Gentry 2011). The bending moment of Series-B was measured 14% higher than the bending moment of 5ply (thickness: 175 mm) CLT by the limit state design method specified in

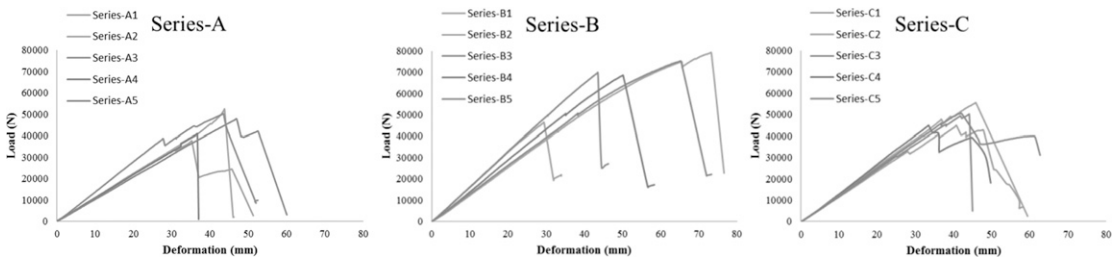


Figure 9. Load–global deformation curves of cross-laminated timber floors.

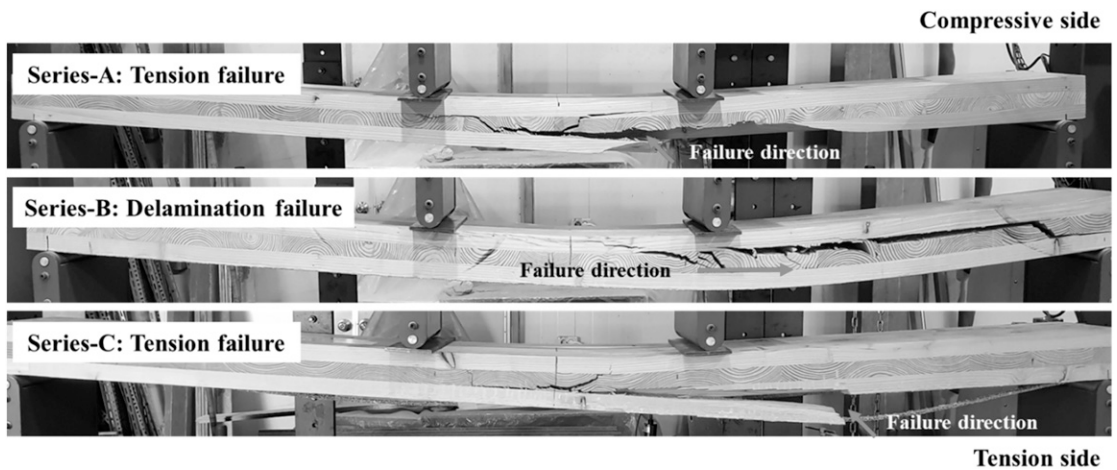


Figure 10. Failure modes of cross-laminated timber (CLT) floor and composite CLT floors.

PRG-320 (PRG 320 2018). In other words, the bending design standard was satisfied even when the amount of wood was decreased by 40% compared with 5ply CLT. The MOE_{Global} and MOR of Series-C, which was reinforced with CFRP bar by machining grooves at regular intervals on the outer surface of the tension member, were 11,621.6 MPa and 41.5 MPa, respectively, which were higher by 9% for MOE and 8% for MOR than those of Series-A. The reinforcement effects were not large, but they will increase if the cross section of the CFRP bar is increased. The mean EI_{Global} of each series

was $2.96 \times 10^{11} \text{ N}\cdot\text{mm}^2$ (Series-A), $3.76 \times 10^{11} \text{ N}\cdot\text{mm}^2$ (Series-B), and $3.22 \times 10^{11} \text{ N}\cdot\text{mm}^2$ (Series-C). Thus, Series-B showed the highest performance. MOE_{Global}/MOE_{Local} and EI_{Global}/EI_{Local} were 0.89, 0.90, and 0.88, respectively, showing no significant difference among the series.

Failure mode. Two failure modes occurred in the bending test: tension failure and delamination failure. In the case of tension failure, the outermost tension member at the center of the specimen begins to fail at the maximum load and

Table 3. Bending strength properties of CLT floors and composite CLT floors.

Series	M.C. (%)	MOE_{Global} (MPa)	MOE_{Local} (MPa)	MOR (MPa)	EI_{Global} (N·mm ²)	EI_{Local} (N·mm ²)	Failure mode
A1	11.8	10,171.5	10,993.5	31.9	2.82×10^{11}	3.04×10^{11}	Tension and rolling shear
A2	11.5	10,471.3	11,764.0	44.2	2.90×10^{11}	3.26×10^{11}	Tension and rolling shear
A3	13.1	12,977.3	14,912.6	42.4	3.59×10^{11}	4.13×10^{11}	Tension and rolling shear
A4	8.8	10,193.1	11,640.3	34.4	2.82×10^{11}	3.22×10^{11}	Tension and rolling shear
A5	13.0	9652.6	10,856.3	40.2	2.67×10^{11}	3.01×10^{11}	Tension and rolling shear
B1	8.1	15,010.5	17,709.2	39.1	4.16×10^{11}	4.90×10^{11}	Delamination and rolling shear
B2	9.8	11,905.4	12,962.4	66.8	3.30×10^{11}	3.59×10^{11}	Delamination and rolling shear
B3	9.9	15,275.5	16,999.7	59.0	4.23×10^{11}	4.71×10^{11}	Delamination and rolling shear
B4	13.7	13,468.9	14,599.8	57.9	3.73×10^{11}	4.04×10^{11}	Delamination and rolling shear
B5	11.9	12,308.0	13,467.5	63.5	3.41×10^{11}	3.73×10^{11}	Delamination and rolling shear
C1	8.7	10,876.7	12,682.3	37.8	3.01×10^{11}	3.51×10^{11}	Tension and rolling shear
C2	8.6	12,049.5	13,760.7	46.9	3.34×10^{11}	3.81×10^{11}	Tension and rolling shear
C3	8.0	11,279.8	12,240.3	42.4	3.12×10^{11}	3.39×10^{11}	Tension and rolling shear
C4	9.6	12,276.2	14,156.6	37.9	3.40×10^{11}	3.92×10^{11}	Tension and rolling shear
C5	9.3	11,625.8	13,022.1	42.7	3.22×10^{11}	3.60×10^{11}	Tension and rolling shear

CLT, cross-laminated timber; M.C., air-dry MC by high-frequency moisture meter.

the failure progresses along the middle lamina to the compression part. In the case of delamination failure, the outermost tension member does not fail, but rolling shear or tension perpendicular failures occur in the middle layer and it completely failed to the end of the cross section along the adhesive layer.

In previous studies, tension failure occurred when there was a defect such as a knot at the center of the tension members comprising the CLT and the tension members were quarter-swan or rift-swan, when all the annual ring directions on the cross section of the tension members were downward, and when the annual ring directions were mixed. The delamination failure occurred when there was no defect such as knot at the center of the tension members and the annual ring directions of the tension members on the cross section were upward or the outside of the tension member was reinforced (Song and Hong 2018).

In this study, a tension failure occurred in all specimens of Series-A of which the tension members were not reinforced as shown in Fig 10. Similar to the previous studies, most of the failures in the specimens occurred at the finger joint or knot of the tension members within the loading point range. In the case of Series-C, even though it was reinforced with CFRP bars, a tension failure occurred as in Series-A. Thus, there was almost no reinforcement effect on the tension member. A delamination failure occurred in the specimens of Series-B of which the entire outside of the tension member was reinforced with CFRP. Even though the tension layer contained defects such as longitudinal joints and knots as in Series-A and Series-C, the tension members of all specimens did not fail, confirming a positive reinforcing effect.

CONCLUSIONS

This study achieved sufficient bonding performance between CFRP and CLT and confirmed that reinforcement using CFRP can greatly contribute to the lightweight and bending performance of the CLT floor. The major conclusions of this study can be summarized as follows.

1. The lowest delamination was measured when the type 1 PUR adhesive was used at the press pressure of 1.0 MPa and adhesive spread of 300 g/m² between CLT and CFRP.
2. When the outside surface of the tension member of the CLT floor was reinforced with a CFRP plate, the MOE_{Global} and MOR increased by 27% and 48%, respectively, than those of the unreinforced CLT. This CFRP composite CLT floor showed a bending performance higher by 14% than the bending moment design value of CLT (5ply) by LSD specified in PRG-320, although its weight was reduced by 40% than 5ply CLT produced with laminae of the same thickness.
3. The reinforcement of CLT by CFRP plate positively suppressed failures caused by defects such as knots on the tension member and longitudinal joints of laminae.

ACKNOWLEDGMENTS

This research was supported by a grant (18RERP-B082884-05) from Residential Environment Research Program funded by the Ministry of Land, Infrastructure and Transport of Korean government.

REFERENCES

- ANSI/APA PRG 320 (2018) Standard for performance-rated cross laminated timber. APA—The Engineered Wood Association, Tacoma, WA.
- Buck D, Wang X, Hagman O, Gustafsson A (2016) Bending properties of cross laminated timber (CLT) with 45° alternating layer configuration. *BioResources* 11(2): 4633-4644.
- Choi C, Yuk CR, Yoo JC, Park JY, Lee CG, Kang SG (2015) Physical and mechanical properties of cross laminated timber using plywood as core layer. *J Korean Wood Sci Technol* 43(1):86-95.
- EN 16351 (2015) Timber structures-cross laminated timber-requirements. Draft version, European Committee for Standardization (CEN).
- Flaig M, Blaß HJ (2014) Bending strength of cross laminated timber beams loaded in plane. *Proc. 13th World Conference on Timber Engineering WCTE 2014*, Quebec City, Canada, August 10-14, 2014.
- Gentry TR (2011) Performance of glued-laminated timbers with FRP shear and flexural reinforcement. *J Compos Constr* 15:861-870.

- Gong Y, Wu G, Ren H (2016) Block shear strength and delamination of cross-laminated timber fabricated with Japanese larch. *BioResources* 11(4):10240-10250.
- Gülzow A, Richter K, Steiger R (2011) Influence of wood moisture content on bending and shear stiffness of cross laminated timber panels. *Eur J Wood Wood Prod* 69: 193-197.
- He M, Sun X, Li Z (2018) Bending and compressive properties of cross-laminated timber (CLT) panels made from Canadian hemlock. *Constr Build Mater* 185:175-183.
- Hochreiner G, Füssl J, Eberhardsteiner J (2014) Cross-laminated timber plates subjected to concentrated loading experimental identification of failure mechanisms. *Strain* 50:68-81.
- Kim KH (2012) Bolted connection strength of glass fiber reinforced glulam. PhD thesis, Department of Wood Science and Engineering, Kangwon National University, Chuncheon, Republic of Korea.
- Kim HK, Oh JK, Jeong GY, Yeo HM, Lee JJ (2013) Shear performance of PUR adhesive in cross laminating of red pine. *J Korean Wood Sci Technol* 41(2):158-163.
- KS F 2160 (2013) Determination of resistance to soaking delamination for adhesive bonded wood products. Korean Standards Association, Seoul, Republic of Korea.
- KS F 3021 (2013) Structural glued laminated timber. Korean Standards Association, Seoul, Republic of Korea.
- Liao Y, Tu D, Zhou J, Zhou H, Yun H, Gu J, Hua C (2017) Feasibility of manufacturing cross-laminated timber using fast-grown small diameter *Eucalyptus* lumbers. *Constr Build Mater* 132:508-515.
- Lu Z, Zhou H, Liao Y, Hu C (2018) Effects of surface treatment and adhesives on bond performance and mechanical properties of cross-laminated timber (CLT) made from small diameter *Eucalyptus* timber. *Constr Build Mater* 161:9-15.
- Okabe M, Yasumura M, Kobayashi K, Fujita K (2014) Prediction of bending stiffness and moment carrying capacity of sugi cross-laminated timber. *J Wood Sci* 60: 49-58.
- Park HM, Fushitani M, Byeon HS, Yang JK (2016) Static bending strength performances of cross-laminated wood panels made with six species. *Wood Fiber Sci* 48(2):1-13.
- Park JC (2009) Strength properties of hybrid fiber-reinforced-plastic reinforced glulam beams. PhD thesis, Department of Wood Science and Engineering, Kangwon National University, Chuncheon, Republic of Korea.
- Rafferty GM, Harte AM (2011) Low-grade glued laminated timber reinforced with FRP plate. *Compos B Eng* 42: 724-735.
- Sikora KS, McPolin DO, Harte AM (2016) Effects of the thickness of cross-laminated timber (CLT) panels made from Irish Sitka spruce on mechanical performance in bending and shear. *Constr Build Mater* 116:141-150.
- Song YJ (2018) Evaluation for mechanical properties of larch CLT and structural strength of CLT wall. PhD thesis, Department of Forest Biomaterials Engineering, Kangwon National University, Chuncheon, Republic of Korea.
- Song YJ, Hong SI (2016) Evaluation of bonding strength of larch cross-laminated timber. *J Korean Wood Sci Technol* 44(4):607-615.
- Song YJ, Hong SI (2018) Performance evaluation of the bending strength of larch cross-laminated timber. *Wood Res* 63(1):105-116.
- Steiger R, Gülzow A, Czaderski C, Howald T, Niemz P (2012) Comparison of bending stiffness of cross-laminated solid timber derived by modal analysis of full panels and by bending tests of strip-shaped specimens. *Eur J Wood Wood Prod* 70:141-153.
- Wang Z, Gong M, Chui YH (2015) Mechanical properties of laminated strand lumber and hybrid cross laminated timber. *Constr Build Mater* 101:622-627.
- Yin X (2018) The seismic behavior of cross-laminated-timber composite slab in high-rise building. *Int J Eng Technol* 10(4):325-328.